Digest Journal of Nanomaterials and Biostructures Vol. 6, No 4, October-December 2011, p. 1639-1647

BIOCOMPATIBILITY STUDY OF EUROPIUM DOPED CRYSTALLINE HYDROXYAPATITE BIOCERAMICS

C.S. CIOBANU[a,b], F. MASSUYEAU[c], E. ANDRONESCU[b], M.S. STAN[d], A. DINISCHIOTU[d], D. PREDOI[a*]

[a]*National Institute for Physics of Materials, 105 bis Atomistilor, P.O. Box MG 07, 077125, Bucuresti-Magurele, Romania,*[*]*Telephone: +40213690185, Fax: +40213690177,*

[b]*University POLITEHNICA of Bucharest, Faculty of Applied Chemistry and Materials Science, Department of Science and Engineering of Oxide Materials and Nanomaterials, 1-7 Polizu Street, P.O. Box 12-134, 011061 Bucharest, Romania*

[c]*Institut des Matériaux-Jean Rouxel, 02 rue de la Houssinière BP 32 229, 44 322 Nantes, France*

[d]*Department of Biochemistry and Molecular Biology, University of Bucharest, 76201, Bucharest , Romania*

For the first time we presented the preliminary results of biocompatibility studies on bioceramic hydroxyapatite powders doped with europium $Ca_{10-x}Eu_x(PO_4)_6(OH)_2$, with $0.01 \leq x_{Eu} \leq 0.2$ prepared at low temperature by a simple coprecipitation approach. The X-ray diffraction (XRD) studies revealed the characteristic peaks of hydroxyapatite in each sample. No evidence for additional crystalline phases was found, proving the complete substitution of Eu in the HAp lattice in the whole range of concentrations. The scanning electron microscopy (SEM) observations suggest that these materials present a little different morphology, which reveals a homogeneous aspect of the synthesized particles for all samples. The PL investigations shown the PL intensity changed considerably by varying the x_{Eu}. The value of x_{Eu} in the hydroxyapatite formula has almost no effect on the wavelength of emission peaks. In order to test Hap_Eu biocompatibility, the effect of europium substituted hydroxyapatite nanocristalline powders with different x_{Eu} on cell viability and proliferation of HEK293 cell line were evaluated. The in vitro investigation showed no significant decrease of viability of HEK293 cell line and low levels of intracellular lipid peroxidation in the Hap_Eu treated cells. In conclusion, the results suggest that Eu doped HAp has low toxicity and exhibit a good biocompatibility.

(Recieved October 3, 2011; accepted October 19, 2011)

Keywords: Europium, Hydroxyapatite, Nanopowder, Byocompatibility

1. Introduction

During the past few years great efforts have been made in order to develop new composites with a large field of application. Because of the numerous and interesting properties bioceramic materials have been the object of intense studies [1,2].

Apatites with a general formula of $M_{10}(TO_4)_6X_2$, where M is a mono,di- or tri-valent cation such as Na^+, Sr^{2+} and La^{3+}; TO_4 a di-, tri- or a tetra-valent anionic group SO^{2-}, VO_4^{3-}, SiO_4^{4-} and X is a mono- or di-valent anion F^-, Cl^-, O^{2-}, S^{2-} are widely spread in studies concerning bone repair and drug delivery systems[3]. Due to the fact that its composition is present in teeth and bones, the most studied compound from apatite's family is hydroxyapatite. HAp having the

[*]Corresponding author: dpredoi@gmail.com

formula $Ca_{10}(PO_4)_6(OH)_2$, has considerably biomedical applications due to its mechanical properties and to the considerably properties of similarity with the mineral constituents of human bone and teeth [4]. It has a hexagonal structure with $P6_3/m$ space group and cell dimensions of a = b = 9.42 Å and c = 6.88 Å. More than that, synthetic HAp has given promising results in the area of drug storage/release and damaged bone reconstruction. Intensive studies have shown incredible biocompatibility, osteoconductivity , non-toxic properties and non-inflamatory properties[5-9]. During the last decade a lot of work was invested in production of synthetic "substituted apatites" using methods such as introducing additional ionic species during the precipitation process in order to improve the materials properties [10-14]. The hydroxyapatite structure oferes a wide range of possible cationic substitution. The cationic substitutions create new composites with potential application in fields such as water purifications, bone pathologies, bioceramics, catalysis and luminescence [15].

During recent years a lot of efforts have been made for achievement of novel biological luminescent nanocrystals and fluorescent biological labels for medical diagnostics and targeted therapeutics applications.

One of the most significant development in the area of luminescent properties was the use of europium as dopant for hydroxyapatite . Eu^{3+} emits in the red region of the visible spectrum and by comparison with other rare earth ions , the Eu^{3+} are used as a local structure probe due to their simple electronic energy level scheme and hypersensitive transition.So far the studies of this kind of biomaterial shown great potential in achieving a very high quality biological probe. [15-17].

In this paper we investigate the doped hydroxyapatite $Ca_{10-x}Eu_x(PO_4)_6(OH)_2$, $0.01 \leq x_{Eu} \leq 0.2$ nancristalline powders and the influence of the x_{Eu} on the structure, morphology, optical properties and biological properties. Europium doped hydroxyapatite with $0.01 \leq x_{Eu} \leq 0.2$ were synthesized by co-precipitation method at 100°C mixing $Eu(NO_3)_3{\cdot}6H_2O$, Ca $(NO_3)_2{\cdot}4H_2O$ and $(NH_4)_2HPO_4$ in deionizated water. The structure, morphology, vibrational and optical properties of the obtained samples were systematically characterized by X-ray diffraction (XRD), scanning electron microscopy (SEM), The biological properties of the $Ca_{10-x}Eu_x(PO_4)_6(OH)_2$ were also investigated.

The biocompatibility tests are presented for the first time. In the present study, the human embryonic kidney cell line (HEK293) was selected as an in vitro model to assess Hap Eu nanotoxicity and biological properties. To test the biocompatibility of europium substituted hydroxyapatite nanocristalline powders, a series of parameters including cell viability, mitochondrial function (MTT assay) was assayed.

2. Experimental

2.1. Sample preparation

All the reagents for synthesis including ammonium dihydrogen phosphate $[(NH_4)_2HPO_4]$, calcium nitrate $[Ca(NO_3)_2{\cdot}4H_2O]$, and europium nitrate $[Eu(NO_3)_3{\cdot}6H_2O]$ (Alpha Aesare) were used as purchased, without purification.

$Ca_{10-x}Eu_x(PO_4)_6(OH)_2$, $0.01 \leq x_{Eu} \leq 0.2$ nanoparticles was performed by setting the atomic ratio of Eu/(Eu + Ca) at 0% (HAp) and 20% (HAp_E20) and (Eu + Ca) /P as 1.67. The $Eu(NO_3)_3{\cdot}6H_2O$ and $Ca(NO_3)_2{\cdot}4H_2O$ were dissolved in deionised water to obtain 300 ml (Ca+Eu) – containing solution. On the other hand the $(NH_4)_2HPO_4$ was dissolved in deionised water to make 300 ml P- containing solution. The (Eu + Ca) – containing solution was put into a Berzelius and stirred at 100°C during 30 minutes. Meanwhile the pH of P- containing solution was adjusted to 10 with NH_3 and stirred continously for 30 minutes. The P- containing solution was added drop by drop into the (Eu + Ca) – containing solution and stirred for 2h and the pH was constantly adjusted and kept at 10 during the reaction. After the reaction the deposited mixtures were washed several times with deionised water. The resulting material was dried at 100°C for 72h.

2.2. Sample characterization

X-ray diffraction (XRD). The samples were characterized by X-ray diffraction using a Bruker D8-Advance X-ray diffractometer, in powder setting, equipped with copper target X-ray tube, Ni filter, and a high efficiency linear detector of Lynx Eye type, operated in integration mode. The patterns were scanned in the 2θ range 15 – 70^o, with a step size of 0.02^o and 36 s measuring time per step.

Scanning electron microscopy (SEM). The structure and morphology of the samples were studied using a HITACHI S2600N-type scanning electron microscope (SEM), operating at 25kV in vacuum. The SEM studies were performed on powder samples.

Photoluminescence PL. Steady-state photoluminescence PL spectra are collected from the front-face geometry of the samples with a Jobin-Yvon Fluorolog spectrometer using a Xenon lamp (500 W) as an excitation source.

Assessment of cytotoxicity. Mitochondrial function and cell viability were measured by the MTT assay [18]. HEK293 cells were plated into a 96-well plate at a density of 5.0 x 10^4 cells/ cm^2. After synchronization, the cells were incubated with 0%, 1%, 2% and 20% of Europium doped hydroxyapatite at all the seven concentrations for 24 respectively 48 hours. The medium from each well was removed by aspiration, the cells were washed with 200µl phosphate buffer saline solution (PBS) per well and then 50µl (1mg/ml) 3-(4,5-dimethylthiazol-2-yl)-2,5-diphenyltetrazolium bromide (MTT) solution was added on each well. After 2 hours of incubation at 37^{o}C the MTT solution from each well was removed by aspiration. A volume of 50µl isopropanol was added and the plate was shaken to dissolve formazan crystals. The optical density at 595 nm, for each well, was then determined using a Tecan multiplate reader (Tecan GENios, Grödic, Germany). The absorbance corresponding to the wells with control cells was used as the 100% viability value.

Lipid peroxidation measurement. Malondialdehyde (MDA) as an *in vitro* marker of lipid peroxidation was assessed by a method described by Del Rio et al. (2003) [19]. At 200 µl of sample with a protein concentration of 2mg/mL protein 700 µl 0.1 N HCl were added and the mixture was incubated for 20 minutes at room temperature. Then, 900 µl of 0.025 M 2-thiobarbituric acid (TBA) were added and the total volume was incubated for 65 minutes at 37°C. Finally 400 µl of 10 mM PBS was added. The fluorescence of MDA was recorded using a 520/549 (excitation/emission) filter. A calibration curve with MDA in the range 0.05-5 µM was used to calculate the MDA concentration. The results were expressed as nmoles of MDA/ mg protein.The total protein concentration was measured by the Bradford method [20] using bovine serum albumin as standards.

3. Results and discussions

The XRD analysis (**Figure 1**) revealed the characteristic peaks of hydroxyapatite in each sample (ICDD file no. 9-432). It is obvious that all the XRD diffractions can by well indexed as a pure hexagonal phase ($P6_3m$ space group). No evidence for additional crystalline phases was found, proving the complete solubilization of Eu in the HAp lattice in the whole range of concentrations. As the Eu concentration increases the peaks broaden, showing that the doping causes lattice perturbation and/or the inhibition of HAp crystal growth. The samples with 1% and 2% Eu are almost identical from XRD point of view with the undoped HAp, showing very small differences concerning the relative intensities of the peaks. As the Eu concentration increases to 20% the peaks broaden, suggesting that the doping inhibits the HAp crystal growth and/or causes lattice perturbations (microstrain). One can observe also an increased background intensity in this pattern, which is presumably due to an amorphous component. The XRD analysis using the anisotropic microstructure analysis implemented in MAUD as “Popa rules” [**21**], gave/provided an average crystallite sizes of around 20 nm in the undoped Hap, and around 7 nm in Hap_Eu20.

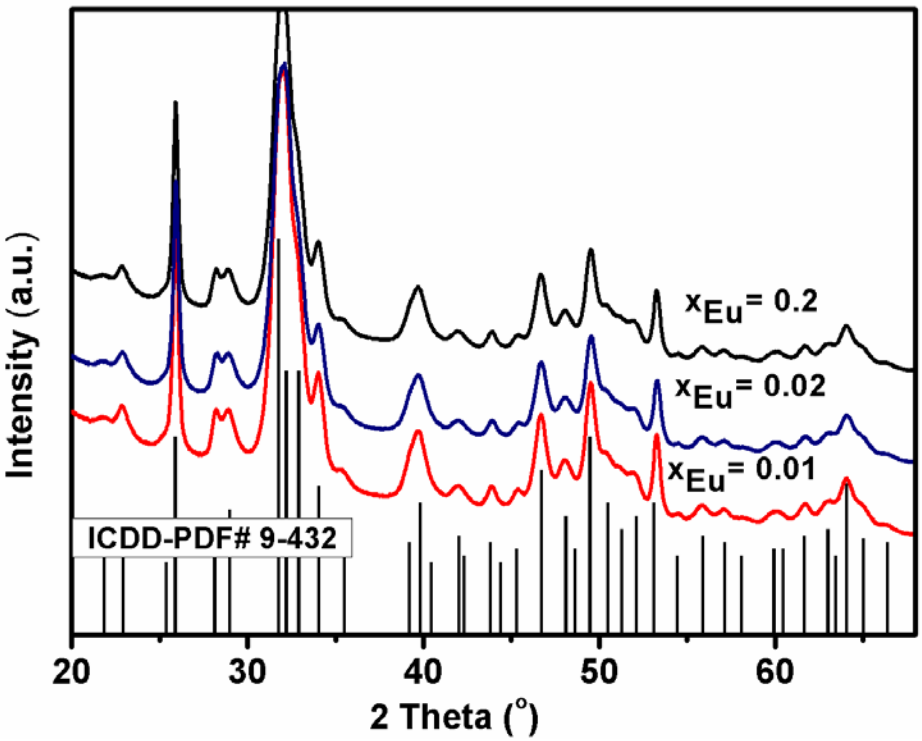

Fig. 1. The XRD patterns of HAp and EuHAp samples synthesized with $0.01 \leq x_{Eu} \leq 0.2$.

SEM images provide the direct information about the size and typical shapes of the prepared samples. It is found that all the samples EuHAp consist of relatively uniform ellipsoidal particles. The result suggests that the doping Eu^{3+} has little influence on the morphology. These materials present a little different morphology, which reveals a homogeneous aspect of the synthesized particles for all samples. **Figure 2** shown the phase maps based on selected region of the sample EuHAp with $0.01 \leq x_{Eu} \leq 0.2$ and simultaneous distributions of individual elements. In **figure 2** the mapping region studied show a uniform of constituent elements.

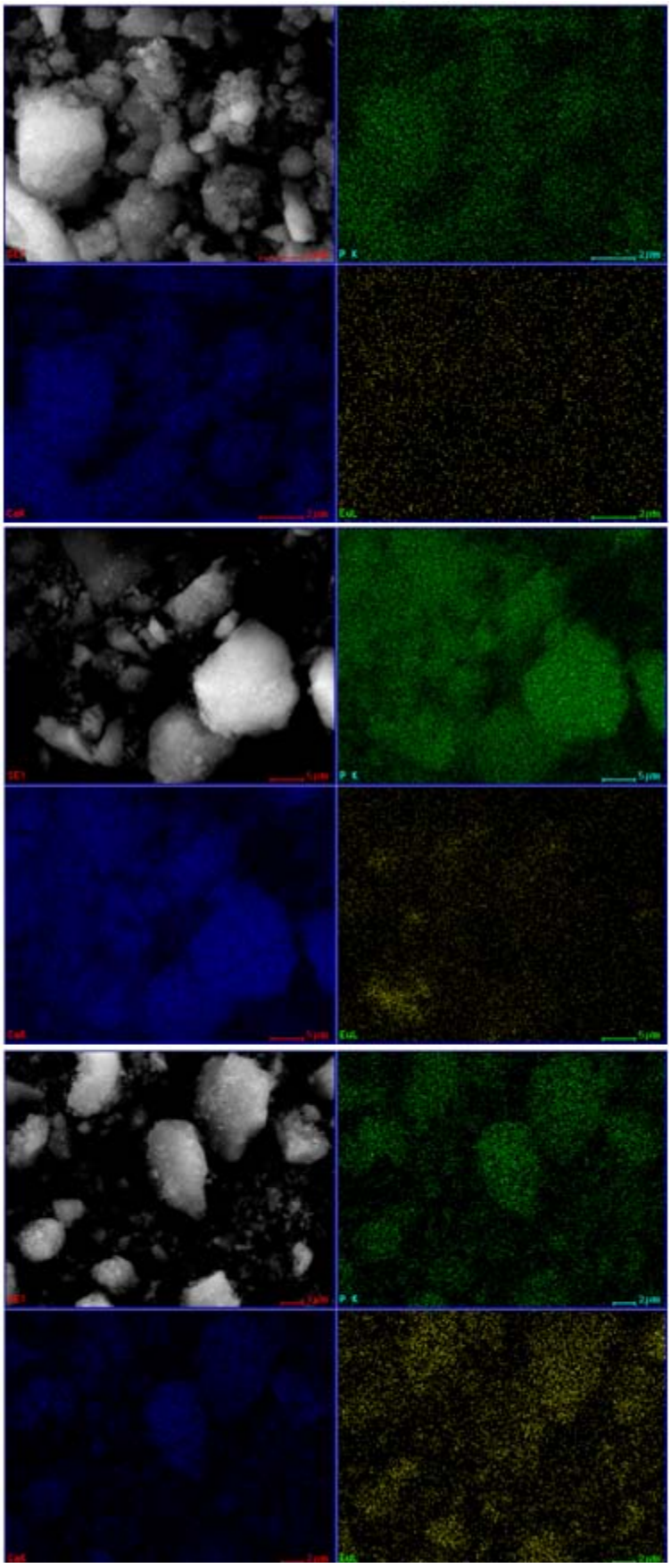

Fig. 2: The phase maps based on selected region of the sample EuHAp with $0.01 \leq x_{Eu} \leq 0.2$ and simultaneous distributions of individual elements.

PL excitation and emission spectra of the EuHAp nanopowders at room temperature are obtained using excitation wavelengths of 395 nm. The excitation and emission spectra are shown in **Figure 4**. In **Figure 3** we shown that the ration Eu/(Ca+Eu) had almost no effect on the wavelength of emission peaks, but the PL intensity changed considerably by varying the atomic ratio Eu/(Ca+Eu). Spectral features are observed in three different ranges: 570–582, 582–603 and 603–640 nm [22]. All the peaks corresponds to typical transitions attributed to to Eu^{3+} ions distributed on Ca^{2+} sites of the apatitic structure [23]. Thus, the emission peaks observed correspond to the $^5D_0 \rightarrow {}^7F_0$ at 578 nm [24], $^5D_0 \rightarrow {}^7F_1$ at 591 nm and 595 nm [25], and $^5D_0 \rightarrow {}^7F_2$ transitions at 614 nm and 618 nm [25]. The most intense peak at 614 nm corresponds to the $^5D_0 \rightarrow {}^7F_2$ tranzition within Eu^{3+} ions. Therefore, the excitation spectrum was obtained by the Eu^{3+} $^5D_0 \rightarrow {}^7F_2$ transition at 614 nm. In these excitation spectra some sharp peaks originating from the f-f transitions of Eu^{3+} can be observed at 300 nm [26]. The highest excitation peak are observed at 250 nm and 394 nm, in the UV region. Beside, excitation in the visible region is possible at 464 nm. The broad peak at 250 nm was attributed to a charge tranfer transition between Eu^{3+} and O^{2-} [27].

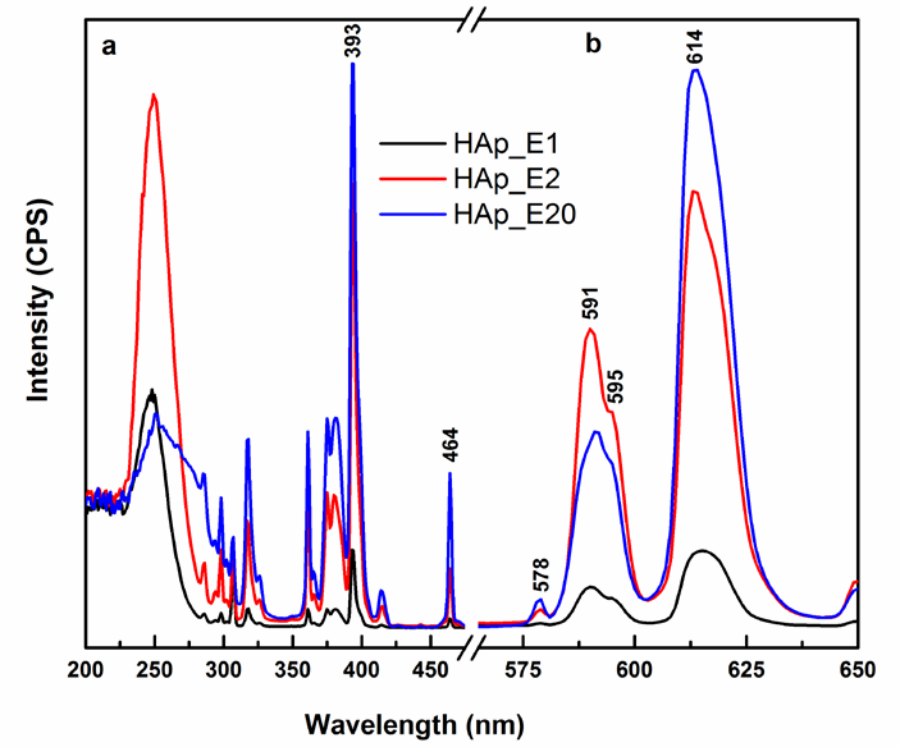

Fig. 3. Excitation(a) and emission(b) spectra of the EuHAp samples synthesized with $0.01 \leq x_{Eu} \leq 0.2$.

In this study we have used HEK 293 cell line due to the fact that it has been well characterized for its relevance to the toxicity models in human [28]. After 48 hours, a decrease in the mitochondrial activity in HEK293 cells exposed to EuHAp samples was observed for x_{Eu} = 0.01 and x_{Eu} = 0.02 at concentrations higher than 5µg/ml, but to a lesser extent. For the treatment by EuHAp (x_{Eu} = 0.2), this diminution was noticed only for the concentrations of 50 and 100 µg/ml.

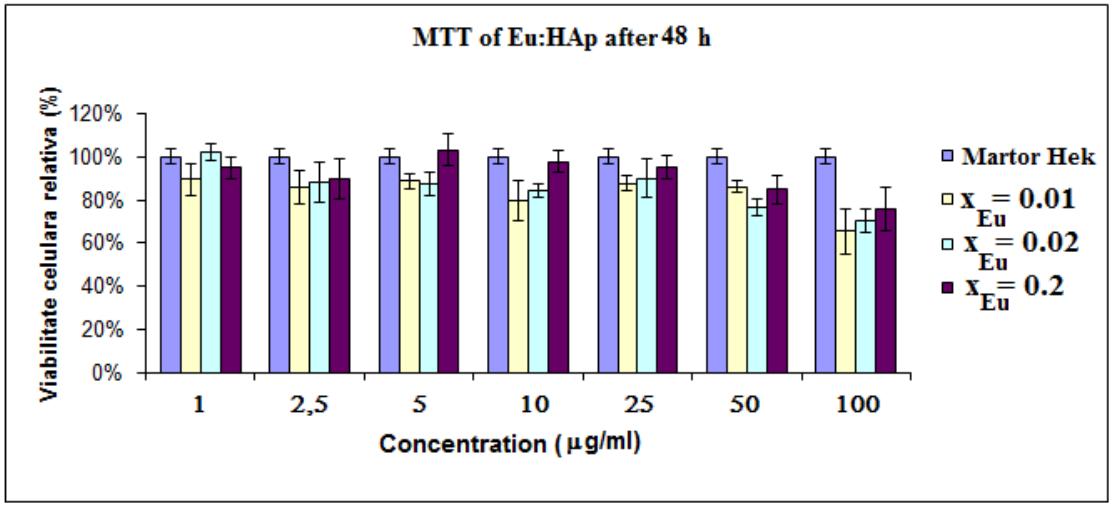

*Fig. 4. The mitochondrial activity of HEK293 cells after 48 h exposure to different concentrations of Europium doped hydroxyapatite nanocristalline powders by MTT assay. Control cells cultured in HAp-free medium were run in parallel to the treated groups. Data are presented as the average ± SD for n = 5. Significance indicated by: *p < 0.05, ** p < 0.01, *** p < 0.001 versus control cells.*

We measured the level of MDA, as a marker of potential toxicity in HEK 293 cells exposed to 2.5, 25 and 100µg/ml of EuHAp, with x_{Eu} = 0.01, x_{Eu} = 0.02 and x_{Eu} = 0.2. . After 48 hours, for EuHAp with x_{Eu} = 0.01, the lipid peroxidation raised by 22% and 42% for 25 µg/ml respectively 100 µg/ml. In the case of EuHAp with x_{Eu} = 0.02, it increased between 22 and 26% for all three concentrations. Moreover, for EuHAp with x_{Eu} = 0.2, MDA level was up regulated by 22%, 24% and 49% for 2.5 µg/ml, 25 µg/ml respectively 100 µg/ml.

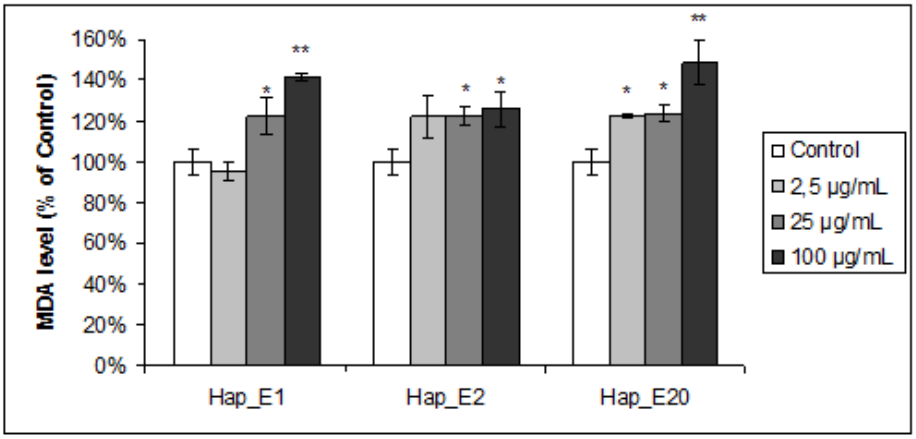

Fig. 5. MDA levels of HEK293 cells after 48 h exposure to three concentrations of Europium doped hydroxyapatite nanocristalline suspensions. Control cells cultured in HAp-free medium were run in parallel to the treated groups. Data are presented as the average ± SD for n = 5.

Significance indicated by: *p < 0.05, ** p < 0.01, *** p < 0.001 versus control cells.

In conclusion, we have carried our study of the atomic ratio of Eu/(Ca+Eu) on the structural, morphological and vibrational properties of hydroxyapatite nanocristalline powders. The XRD studies have shown that the characteristic peaks of hydroxyapatite in each are presented. No evidence for additional crystalline phases was found, proving the complete ssubstitution of Eu in the HAp lattice in the whole range of concentrations. The samples with $0.01 \leq x_{Eu} \leq 0.02$ are almost identical from XRD point of view with the undoped HAp, showing very small differences concerning the relative intensities of the peaks. As the atomic x_{Eu} increases to 0.2 the peaks

broaden, suggesting that the doping inhibits the HAp crystal growth and/or causes lattice perturbations (microstrain). Differences in the luminescence spectra between HAp_E1 (x_{Eu}= 0.01), HAp_E2(x_{Eu}= 0.02) and HAp_E20(x_{Eu}= 0.2) powders are not attributable to variations in morphology, as the powders are similar in shape. These studies demonstrate that luminescent Eu^{3+} doped hydroxyapatite represents a potential application for drug release and targeting based on their luminescent properties. For the first time we presented the preliminary results of biocompatibility studies. This studies suggests that exposure to Europium doped hydroxyapatite nanocristalline powders did not dramatically decreased HEK-293 cell viability as indicated by mitochondrial function and intracellular lipid peroxidation levels. The results support the idea that the tested materials exhibit good biocompatibility and are safe to use.

Acknowledgements

The work has been funded by the Sectoral Operational Programme Human Resources Development 2007-2013 of the Romanian Ministry of Labour, Family and Social Protection through the Financial Agreement POSDRU/6/1.5/S/19.

References

[1] K. de Groot, Biomaterials **1**, 47(1980).
[2] F.C.M. Driessens, in: K. de Groot (Ed.), Bioceramic of Calcium Phosphate, CRC Press, Boca Raton, FL (1983).
[3] E. Boanini, M. Gazzano, A. Bigi. Acta Biomaterialia **6**, 1882(2010).
[4] N.C. Popa, J. Appl. Cryst. **31,** 176(1998).
[5] A. Costescu, I. Pasuk, F. Ungureanu, A. Dinischiotu, M. Costache, F. Huneau, S. Galaup, P. Le Coustumer, D. Predoi, Digest Journal of Nanomaterials and Biostructures **5**(4), 989(2010).
[6] C. S. Ciobanu, E. Andronescu, A. Stoicu, O. Florea, P. Le Coustumer, S. Galaup, A. Djouadi, J.Y. Mevellec, I. Musa, F. Massuyeau, A. M. Prodan, K. Lafdi, R. Trusca, I. Pasuk, D. Predoi, Digest Journal of Nanomaterials and Biostructures **6**(2), 609(2011).
[7] C. S. Ciobanu, E. Andronescu, B. S. Vasile, C. M. Valsangiacom, R. V. Ghita, D. Predoi, Optoelectron. Adv. Mater.-Rapid Comm. **4**(10), 1515(2010).
[8] D. Predoi,S. Derible, H. Duflo, J. Optoelectron. Adv. Mater. **11**(6), 852(2009).
[9] D. Predoi, R.A. Vatasescu-Balcan, I. Pasuk, R. Trusca, M. Costache, J. Optoelectron. Adv. Mater. **10**(8), 2151(2008).
[10] D.L. Shi, J. Lian, W. Wang, G.K. Liu, P. He, Z.Y. Dong, L. M.. Wang, R. C. Ewing, Adv. Mater. **18**, 189(2006).
[11] R. Ternane, M. Trabelsi-Ayedi, N. Kbir-Ariguib, B. Piriou, J. Lumin. **81,** 165(1999).
[12] M. Gaft, R. Reisfeld, G. Panczer, S. Shoval B. Champagnon, G. Boulon, J. Luminescence, **72-74**, 572(1997).
[13] Predoi, D; M. Barsan, E. Andronescu, R.A. Vatasescu-Balcan M. Costache, J. Optoelectron. Adv. Mater. **9**(11), 3609(2007).
[14] D. Predoi, R.V. Ghita, F. Ungureanu, C.C. Negrila, R.A. Vatasescu-Balcan, M.Costache, J. Optoelectron. Adv. Mater. **9**(12), 3827(2007).
[15] A. Zounani, D. Zambon, J.C. Cousseins, J. Alloys Compd. **188**, 82(1992).
[16] G. Blasse, B.C. Grabmaier, Luminescent materials. Berlin/Heidelberg: Springer-Verlag, (1994).
[17] Y. Wang, X. Guo, T. Endo, Y. Murakami, M. Ushirozawa, J. of Solid State Chem. **177,** 2242(2004).
[18] F. Denizot, R. Lang, CJ Immunol Methods **89**, 271(1986).
[19] D. Del Rio, N. Pellegrini, B. Colombi, M. Bianchi, M. Serafini, F. Torta, M. Tegoni, M. Musci, F. Brighenti, Clinical Chem. **49** (9), 690(2003).
[20] M.M. Bradford, Anal. Biochem **72,** 248(1976).
[21] N.C. Popa, J. Appl. Cryst. **31**, 176(1998).

[22] D.L. Shi, J. Lian, W. Wang, G.K. Liu, P. He, Z.Y. Dong, L. M.. Wang, R. C. Ewing, Adv. Mater. **18**, 189(2006).
[23] R. Ternane, M. Trabelsi-Ayedi, N. Kbir-Ariguib, B. Piriou, J. Lumin. **81,** 165(1999).
[24] M. Gaft, R. Reisfeld, G. Panczer, S. Shoval B. Champagnon, G. Boulon, J. Lumin. **72-74**, 572(1997).
[25] A. Zounani, D. Zambon, J.C. Cousseins, J. Alloys Compd. **188**, 82(1992).
[26] G. Blasse, B.C. Grabmaier, Luminescent materials. Berlin/Heidelberg: Springer-Verlag, (1994).
[27] Y. Wang, X. Guo, T. Endo, Y. Murakami, M. Ushirozawa, J. of Solid State Chem. **177,** 2242(2004).
[28] V.V. Goncharuk, K.A. Nezheradze, E.V. Datskevich, J Water Chem Tech. **32**, 51(2010).